A Small Multi-band MEMS Switched PIFA

K. R. Boyle[1] and P. G. Steeneken[2]

[1]NXP Semiconductors, Research, UK
[2]NXP Semiconductors, Research, The Netherlands

Abstract— This paper presents the design of a small MEMS switched planar inverted F antenna capable of operation in five cellular radio frequency bands. Both simulated and measured results are presented. The MEMs devices used in the measurements are fabricated in an industrialized process based on high-ohmic silicon.

1. INTRODUCTION

Planar inverted F antenna (PIFAs) are widely used in mobile phones. They suffer from a problem that is common to all electrically small antennas — they have limited bandwidth for a given size. This is a constant challenge for antenna designers, since there is a continual trend towards operation within more bands (for global "roaming") and a constant desire to reduce the antenna volume. Figure 1 shows the five UTRA (UMTS Terrestrial Radio Access) FDD and GSM bands used in Europe and America (and also many other countries worldwide).

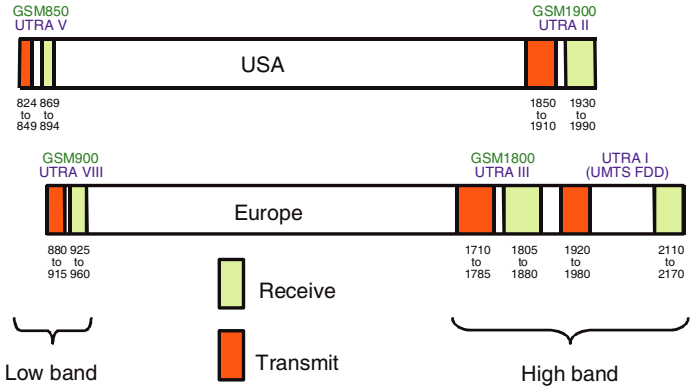

Figure 1: Common cellular frequency bands used in Europe and the USA (MHz).

Simultaneous operation is not required in all bands: the antenna can be switched to operate in a subset of the total number of bands at any given time. However, though MEMS switched antennas have been reported previously [1–3], none have been shown to be capable of operation over five mobile phone frequency bands.

To achieve switching over a bandwidth of approximately one octave without significantly reducing efficiency, high quality microelectromechanical systems (MEMS) switches have been developed [4–7]. Capacitive switches, fabricated in the industrialized Philips PASSI^{TM} process, are reported here.

2. ANTENNA GEOMETRY AND MEMS CIRCUITRY

The antenna geometry and MEMS circuitry is shown in Figure 2. The antenna has dimensions $40 \times 12 \times 8$ mm, whereas the PCB has dimensions $40 \times 100 \times 0.8$ mm and is metalized on the back surface to provide an RF ground. All circuitry is on the PCB rather than the antenna and the slot in the antenna is located such that it is unlikely to be perturbed when the phone is held [8, 9].

The MEMS devices (shown as variable capacitors in Figure 2) require an actuation voltage of between 30 V and 50 V. MEMS Die 1 controls the antenna impedance and Die 2 controls the antenna resonant frequency. The circuit values for each operational mode are given in Table 1. The matching inductor, L1 is fixed and is realized as a meander line on the PCB. L2 is for DC biasing and is realized using a surface mount device (SMD) of value 10 nH. Capacitors CB1 and CB2 are used for DC blocking, whereas CD1-CD4 are for decoupling. All are 200 pF. Finally, resistors R1-R4 have a resistance of 10 kΩ. and are for decoupling the DC actuation voltages of the MEMS switches applied at terminals VDC1-VDC4.

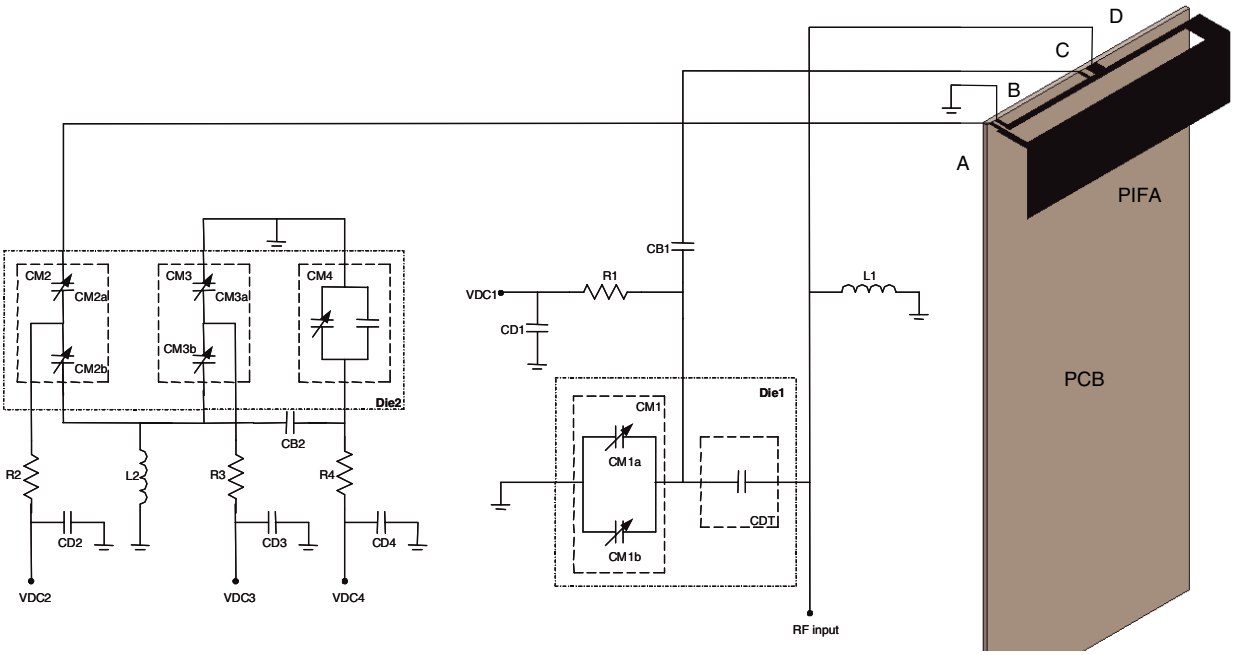

Figure 2: MEMS switched PIFA and circuit.

Table 1: MEMS capacitor values (pF) with operational mode.

Mode	CDT	CM1a CM1b	CM2A CM2B	CM3A CM3B	CM4
GSM850/900	12	10	0.2	3.4	5.7
GSM1800	12	10	4.0	3.4	5.7
GSM1900	12	.5	4.0	3.4	0.57
UMTS	12	.5	4.0	0.17	0.57

The MEMS capacitors CM2 and CM3 are series combinations of two capacitive switches in order both to reduce the OFF state capacitances and to improve voltage handling. CM1 is a parallel combination of two capacitive switches to increase the ON capacitance and CM4 is the combination of a fixed and a MEMS capacitor. CDT is a fixed capacitor that is used to double-tune the antenna in the lowest frequency mode. It is realized on the MEMS die to allow the use of non-preferred values.

3. SIMULATED RESULTS

The antenna and interconnects are modeled using Ansoft HFSS with all component positions represented as lumped ports. This allows a multi-port s-parameter file to be generated and subsequently imported into the Agilent ADS circuit simulator. Components can then be placed at the ports of the s-parameter network and the input impedance, circuit efficiency etc simulated. The simulated impedance in the four operational modes is shown in Figure 3. All modes have are capable of an S_{11} of -6 dB or better (referred to 50 Ohms) — the UMTS mode is deliberately designed to have a resonant frequency that is too high in order to allow DC tuning to lower frequencies.

4. IMPLEMENTATION

A photograph of the MEMS switched antenna is shown in Figure 4.

The antenna is fabricated from a polyimide flexible PCB that is folded over a Rohacell block. The antenna/PCB combination is fed via a coaxial cable at a central point on the PCB to avoid excessive perturbation from the feeding cables [10]. The MEMS capacitors are placed on two dies under the antenna, as shown in Figure 5. It can be seen that the bond wires used to connect from

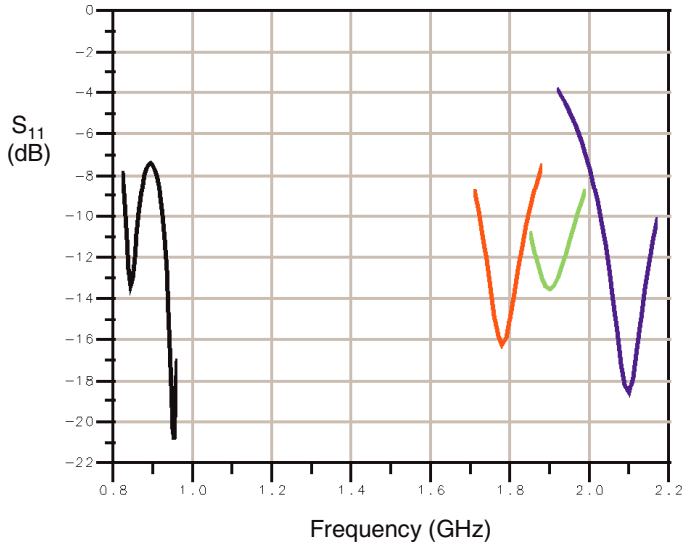

Figure 3: Simulated S_{11}: 824–960 MHz (black), 1710–1880 MHz (red), 1850–1990 MHz (green), 1920–2170 MHz (blue).

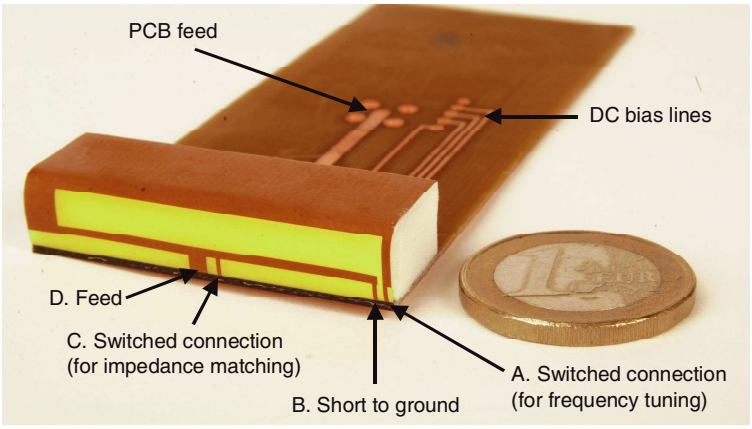

Figure 4: MEMS switched PIFA and PCB.

the MEMS dies to the PCB interconnects are rather long, in part due to the solder used to connect the SMDs. To compensate for device and assembly uncertainties, MEMS devices with slightly varying layouts are implemented.

5. MEASUREMENTS

Measured results are shown in Figure 6.

In the UTRA band V/VIII mode, the S_{11} is below −6 dB between 765–950 MHz, showing that a wide bandwidth resonance is obtained. The centre frequency is somewhat lower than that simulated at 830 MHz, but the bandwidth is approximately 180 MHz (fractionally, 22%), which is slightly better than simulated. For the high frequency bands, the resonant frequencies are somewhat higher than simulated. The −6 dB bandwidths are 1930–2062 MHz, 1941–2071 MHz and 2005–2117 MHz for the UTRA bands III, II and I respectively. These bandwidths are less than simulated. However this is largely due mismatch. With inductive matching, bandwidths of approximately 300 MHz — slightly higher than those simulated — can be achieved. Resonant frequency shifts are clearly observed in the high frequency modes, though the magnitudes of the shifts are less than simulated. The differences between simulation and measurement are attributed predominantly to uncertainties in the capacitance density of the MEMS devices and the long (un-simulated) bond wires used.

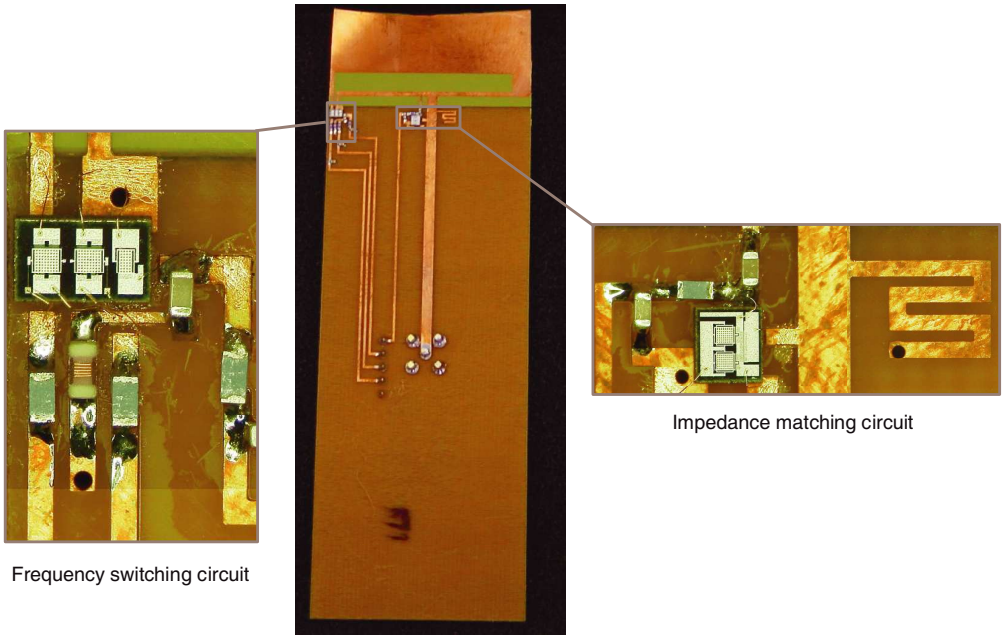

Figure 5: Unfolded antenna and details of MEMS dies and surrounding components.

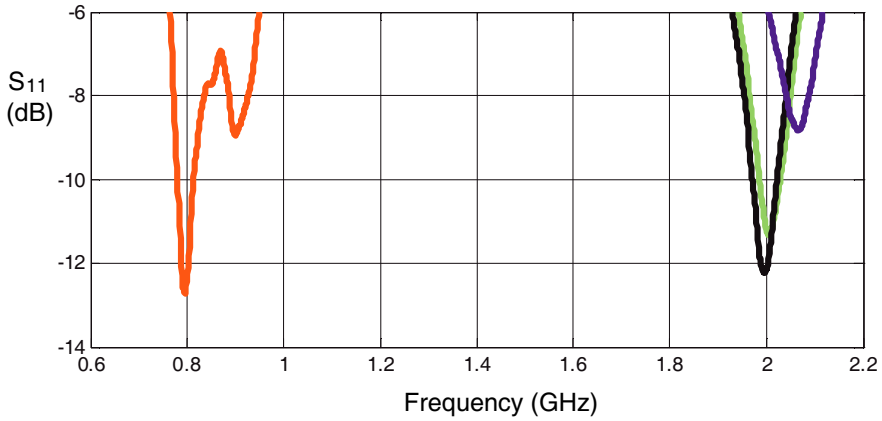

Figure 6: Measured S_{11} (below -6 dB): 765–960 MHz (red), 1930–2062 MHz (black), 1941–2071 MHz (green) and 2005–2117 MHz (blue). Low and high frequency results are measured with slightly different MEMS devices.

6. CONCLUSIONS

A five-band MEMS switched antenna, utilizing capacitive MEMS switches is demonstrated. The measured prototype confirms that the antenna is capable of operating in several modes over a bandwidth of greater than one octave. It is also confirmed that wide bandwidths are feasible (in each mode) from an antenna that is smaller than conventional. In the future, the use of directly soldered, packaged MEMS with improved capacitance density tolerances, will lead to closer agreement between simulations and measurement.

REFERENCES

1. Kiriazi, J., H. Ghali, H. Ragaie, and H. Haddara, "Reconfigurable dual-band dipole antenna on silicon using series MEMS switches," *Proceedings of the IEEE Antennas and Propagation Society International Symposium*, Vol. 1, 403–406, 22–27 June 2003.
2. Panaia, P., C. Luxey, G. Jacquemod, R. Staraj, G. Kossiavas, L. Dussopt, F. Vacherand, and C. Billard, "MEMS-based reconfigurable antennas," *Proceedings of the IEEE International Symposium on Industrial Electronics*, Vol. 1, 175–179, 4–7 May 2004.
3. Onat, S., M. Unlun, L. Alatan, S. Demir, and T. Akin, "Design of a re-configurable dual

frequency microstrip antenna with integrated RF MEMS switches," *Proceedings of the IEEE Antennas and Propagation Society International Symposium*, Vol. 2A, 384–387, 3–8 July 2005.

4. Rijks, T. G. S. M., et al., "Passive integration and RF MEMS: a toolkit for adaptive LC circuits," *Proceedings of the 29th European Solid-State Circuits Conference*, 269–272, 16–18 Sept. 2003.
5. Van Beek, J. T. M., et al., "High-Q integrated RF passives and micromechanical capacitors on silicon," *Proceedings of the Bipolar/BiCMOS Circuits and Technology Meeting*, 147–150, 28–30 Sept. 2003.
6. De Graauw, A. J. M., P. G. Steeneken, C. Chanlo, J. Dijkhuis, S. Pramm, A. van Bezooijen, H. K. J. ten Dolle, F. van Straten, and P. Lok., *Proc. BCTM2006*, 2006.
7. Van Beek, J. T. M., P. G. Steeneken, G. J. A. M. Verheijden, J. W. Weekamp, A. den Dekker, M. Giesen, A. J. M. de Graauw, J. J. Koning, F. Theunis, P. van der Wel, B. van Velzen, and P. Wessels, "MEMS for wireless communication: application, technology, opportunities and issues," *Proceedings of MEMSwave2006*, session 5, paper 17, 2006.
8. Boyle, K. R. and L. P. Ligthart, "Radiating and balanced mode analysis of PIFA antennas," *IEEE Transactions on Antennas and Propagation*, Vol. 54, Issue 1, 231–237, Jan. 2006.
9. Boyle, K. R. and L. P. Ligthart, "Radiating and balanced mode analysis of user interaction with PIFAs," *Proceedings of the IEEE Antennas and Propagation Society International Symposium*, Vol. 2B, 511–514, Washington DC, July 4th–8th, 2005.
10. Massey, P. J. and K. R. Boyle, "Controlling the effects of feed cable in small antenna measurements," *Proceedings of ICAP 2003*, 31 Mar.–3 Apr. 2003.